Clinical Device-Related Article
Bone properties surrounding hydroxyapatite-coated custom osseous integrated dental implants

M. I. Baker,[1] A. W. Eberhardt,[1] D. M. Martin,[2] G. McGwin,[3] J. E. Lemons[4]

[1]Department of Biomedical Engineering, University of Alabama at Birmingham, Birmingham, Alabama
[2]Private Practice, Stockton, 1310 E. Swain Rd., Stockton, California 95210
[3]Department of Epidemiology, University of Alabama at Birmingham, Birmingham, Alabama
[4]Department of Prosthodontics, University of Alabama at Birmingham, Birmingham, Alabama

Received 16 November 2009; revised 28 May 2010; accepted 2 June 2010
Published online 19 August 2010 in Wiley Online Library (wileyonlinelibrary.com). DOI: 10.1002/jbm.b.31693

Abstract: Calcium phosphate (hydroxyapatite or HA) coatings have been applied to Custom Osseous Integrated Implants (COIIs) to improve the quality of the bone-implant integration, yet little is known concerning the biomechanical properties of bone surrounding the HA-coated implants in humans over the long term. The purpose of this study was to characterize the mechanical and histomorphometric properties of the bone along the implant interface. Specimens were prepared from three similar mandibular implants that were functional in three female patients for about 11 years. Histomorphometric analyses showed bone-implant contact averaging 75% for all specimens. Area coverage of residual HA-coating ranged from 52 to 70%. When compared with previous studies, these results show a relatively high percentage of residual HA after a decade *in vivo*. Nanoindentation showed similar average values of hardness and modulus ($p = 0.53$ and $p = 0.56$, respectively) comparing bone adjacent to residual HA-coating and regions where the coating was absent. The elastic modulus was significantly lower for bone near the bone-implant interface (<200 μm) as compared with bone distant (>1000 μm) from the interface ($p = 0.05$), thereby reflecting different properties of the bone near these interfaces. Backscattered electron imaging showed darker gray levels which indicated decreased mineral content in bone adjacent to the implant, consistent with the nanoindentation results. J Biomed Mater Res Part B: Appl Biomater 95B: 218–224, 2010.

Key Words: bone, hydroxyapatite, dental implants, nanoindentation

INTRODUCTION

Dental implants are widely used for replacement of teeth and correction of defects in maxillary and mandibular bone. Their effectiveness is largely dependent upon biological stability and integration between the bone and implant. Surrounding the implant, bone modeling and remodeling results in restructuring of bone tissue around the implant.[1] This integration to bone plays a key role in the fixation and anchoring of the implant. A common cause of dental implant failure is aseptic loosening due to bone loss at the bone-implant interface.[2] To combat such conditions, bioactive coatings, altered surface topographies, and other methods have been employed to enhance integration and stability.[3–6] Studies indicate that coating metallic or ceramic implants with calcium phosphate based compounds (called hydroxyapatite or HA) improves the fixation between bone tissues and implants while minimizing fibrous tissue formation at the interface.[7–9] HA has been shown to be osteoconductive and biocompatible, and has been used to influence implant success rates by promoting more rapid fixation,[2] better bone anchoring,[7–9] and long term stability along the bone-implant interfaces.[10–12]

Previous studies have demonstrated that over the long term some types of hydroxyapatite coatings surrounding an implant may not be retained.[13–16] The loss of the HA-coating has raised concerns regarding potential mechanical instability over time. Studies have shown, however, that bone remodels in direct contact with the metallic implants after loss of HA coating.[17–19] Iezzi et al.[19] reported 78% bone-implant contact in one implant retrieved after 15 years service with almost complete removal of the HA coating, consistent with ongoing integration of the implant. Tonino et al[13] and Carlsson et al[20] reported 22–56% and 20–67% bone implant contact, respectively, in retrieved HA-coated implants with a substantial loss of the coating. Numerous studies have been conducted on prior subperiosteal designs; however, to date, no such studies have been reported on this particular design and clinical approach, called Custom Osseous Integrated Implants (COIIs). This

Correspondence to: J. E. Lemons; e-mail: jlemons@uab.edu
Contract grant sponsor: National Institute of Biomedical Imaging and Bioengineering (NIBIB); contract grant number: RO1 EB001715-01A2
Contract grant sponsor: National Institute of Health (NIH); contract grant number: P30-AR46031
Contract grant sponsors: UAB CMBD Histomorphometry and Molecular Analysis Core Laboratory, UAB Experimental Biomechanics Core

cast form of cobalt alloy was selected to provide a custom fit to the bone, higher elastic modulus (increased stiffness for construct rigidity/stability and distributed force transfer) and similar fatigue strength compared to high quality cast titanium alloy. Also a calcium phosphate based coating on the implant body section was included to promote integration with bone. The selection of cobalt alloy versus other alloy types was based on decades of experience gained from casting many different designs of dental devices from the Co-Cr-Mo alloy. An examination of these three HA-coated COIIs may elucidate factors influencing bone integration and provide insight into parameters of value to the profession at large.

Nanoindentation is a characterization technique with a spatial resolution better than 1 μm,[21] which has been used to measure the mechanical properties of bone at a nanometer level.[21–23] Zysset et al.[23] indented human femora and reported values of elastic modulus that were higher for cortical bone than surrounding trabecular bone. Rho et al.[21] found higher values of nanoindentation modulus for interstitial lamellae when compared to osteonal bone in human tibiae. Hoffler et al.[22] studied the cortical and trabecular bone from the femoral neck and diaphysis, distal radius, and fifth lumbar vertebra and observed greater values of elastic modulus for cortical osteonal, interstitial, and primary lamellae tissue than for trabecular bone within an anatomical location. It is clear, therefore, that the elastic modulus of human bone tissue depends on anatomical location, tissue type, and individual.[23]

Others have characterized the mechanical properties of bone surrounding dental implant devices. Huja et al.[24] studied HA-coated and uncoated threaded endosseous dental implants, which were implanted in the mid-femoral diaphyses of male hounds. They found after 12 weeks *in vivo* that the microhardness increased exponentially at a distance between 200 to 600 μm from the implant-bone interface. Chang et al.[1] studied titanium threaded dental implants in swine alveolar bone and after one month observed a gradient in bone modulus "near" the implant (<200 μm), followed by a plateau, and an increase in modulus at distances greater than 1000 μm. Oyen et al.[25] analyzed the same specimens using a viscous-elastic-plastic indentation model and determined that there was an increase in elastic modulus with increased distance from the bone-implant interface, with no clear trend in hardness. Clark et al.[26] studied bone-implant interface of screw-type titanium implants in rabbit maxilla and femur after one month implantation. Their results in the femur were similar to Chang et al.,[1] and showed an increasing gradient in modulus as a function of distance from the interface. To our knowledge there have been no studies analyzing the mechanical properties using nanoindentation of bone interfaces around long-term HA-coated subperiosteal dental implants in humans.

The aim of this study was to characterize the bone surrounding HA-coated Custom Osseous Integrated Implants (COIIs) that had been in function for relatively long periods of time *in vivo* (>10 years). To achieve this aim, the mechanical and histomorphometric parameters of bone surrounding three similar implants were characterized. The bone-implant contact ratio was calculated to determine the degree of bone integration *in vivo*. The hardness and elastic modulus of bone adjacent to the HA-coated regions was measured using nanoindentation and values near residual HA coatings were compared with those adjacent to the CoCr implant substrates, where HA was absent. It was hypothesized that bone located near the implant's HA interface would display mechanical properties comparable to bone distant from the implant, reflecting stable bone properties for functional implant constructs.

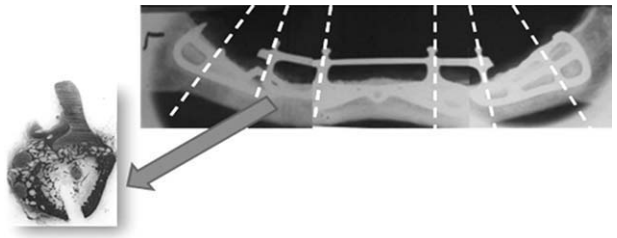

FIGURE 1. Radiographic image of a mandibular custom osseous integrated implant. The dashed lines represent the approximate location where the implant was sectioned. A cross section of one of the sections is also shown.

Backscattered electron (BSE) imaging is a technique used to determine differences in density for surface regions resulting in an image with different gray levels. The higher the density for a specific atomic structure of the mineral phase, the more electrons backscattered from the surface region and the lighter the resulting image.[27] Presently, this technique was used to visualize bone areas of higher or lower density (degree of mineralization) surrounding the implant interface. It was conjectured that these image data would complement the nanoindentation results and provide additional evidence of mature stable bone along the implant interface.

MATERIALS AND METHODS

Sample preparation

Implants were recovered from three female patients post mortem, ages 74–94 years, after being *in vivo* for ~11 years each. The implants were made with ASTM F-75 cast cobalt chromium alloy (CoCr) and plasma sprayed with HA coating.[28] During surgery, HA particulates were placed around the CoCr implants. All three implants were functioning as intended at the time of patient deaths. Laboratory analyses were conducted under IRB approval and in compliance with HIPAA requirements at our institution [IRB# X050823001].

The implant-mandible constructs were sectioned at the anterior and posterior posts for a total of six sections per mandible (Fig. 1). Specimen preparation included controlled dehydration, embedding in methyl methacrylate, sequential polymerizing, grinding under constant water irrigation with silicon carbide paper (320, 800, 1000, and 2500) grit sizes followed by polishing with diamond pastes (3, 0.25 μm) and alumina slurry (0.05 μm). All processed nondecalcified thin sections were stained with methylene blue (Allied Chemicals, NY)/basic fuschin (Sigma-Aldrich, MO) and sonicated with deionized water between grinding and polishing steps and prior to nanoindentation.

Histomorphometric analyses

Histomorphometric analyses were used to determine the percentage of bone in direct contact with the surfaces of the implants. The sections were recut into 70–100 μm thick slides and stained with Sanderson's Bone Stain. Slides were examined by optical microscopy using an Olympus BX51 microscope with a Retiga EXi color digital camera (Olympus, Center Valley, PA) and Bioquant® software (R&M Biometrics, Nashville, TN) at an original magnification of 10×. The histomorphometric parameters measured included "% Bone-HA coating," defined as the interfacial length per total length of mineralized bone in direct contact with the residual HA coating; "% Bone-CoCr," defined as bone in direct contact with the implant where the HA was absent; and "BIC," defined as the total amount of bone-implant contact (including regions were HA was present or absent).

Nanoindentation

Elastic modulus and hardness of bone around the implant sections were measured by nanoindentation (MTS Nano Indenter G200, Oak Ridge, TN). Bone is viscoelastic; therefore, holding times of 100 seconds at maximum depth and 10 s at 90% of the unload depth were used to reduce influences of creep and thermal drift, respectively.[29] Elastic modulus was calculated from the initial unloading portion of the load vs. displacement curve, according to the method of Oliver and Pharr.[17] Fused silica (modulus = 72 GPa) was indented as part of each set of indentations to confirm the reproducibility and accuracy of the testing system. Indentation results were considered valid if the modulus from the associated silica indentations were 72.0 ± 2 GPa.

Indentations were placed along the interface and away from the interface at a spacing of 50 μm. Indents considered "near" were within 200 μm, while "distant" indents were greater than 1000 μm from the interface. The indents performed surrounding the interfaces were separated depending on the location: "bone-HA coating" where the HA-coating was present and "bone-CoCr" where the HA-coating was absent. A cross section of one representative specimen is shown in Figure 1.

Backscattered electron imaging

The same specimens used for nanoindentation were sputter-coated with carbon and used for scanning electron microscopic analyses. Backscattered electron (BSE) imaging perpendicular to the surface was done using the JEOL 7000 scanning electron microscope (SEM, JEOL Ltd, Japan) using a voltage of 20 kV. Representative areas of the implant-bone interface that revealed residual HA coating and/or direct bone-CoCr contact were selected for imaging records.

Statistical analysis

Nanoindentation values (elastic modulus and hardness) were combined under categorizations according to their distance from the interface: <200 μm was classified as "bone-HA coating" and "bone-CoCr" depending on the presence or absence of the HA coating and >1000 μm as bone "distant" to the interface. Linear mixed models were then used to compare nanoindentation values between and among these three groups.

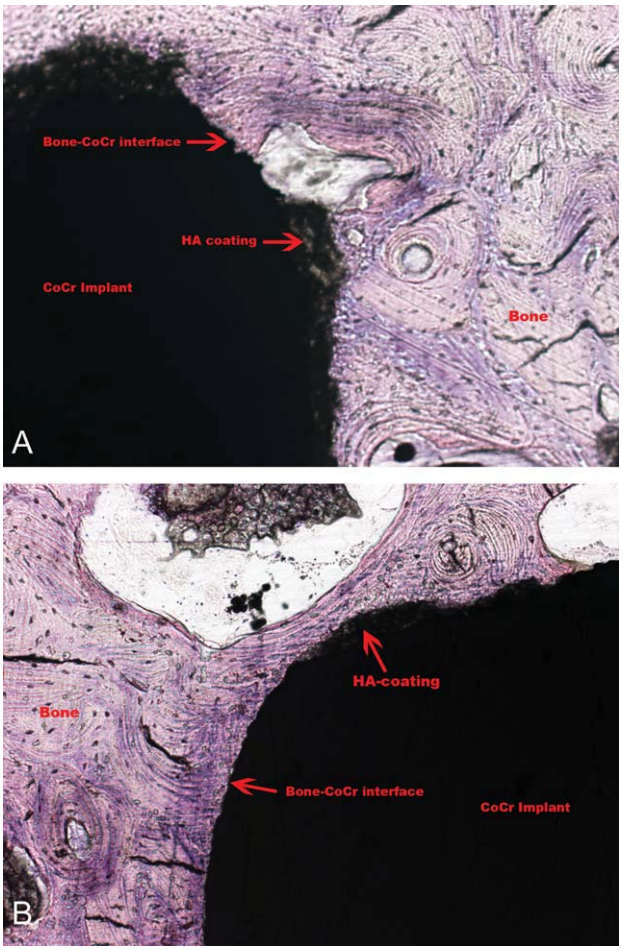

FIGURE 2. A, B: Implant interfaces demonstrating areas of bone-HA-coating contact and bone-CoCr contact. The original HA coating present was directly in contact with bone, while in other areas the coating was missing and bone tissue was in close contact with the implant surface (Sanderson's Bone Stain, original magnification ×10).

RESULTS

Histomorphometric analyses

Histological examination demonstrated that, overall, there was considerable bone-implant integration with no signs of pathology in the analyzed regions for any of the specimens. In some areas the HA coating was absent and the implant surface was covered with anatomically mature, compact-like bone, while other areas showed contiguous bone-HA coating [Figure 2(A,B)]. In some samples, the hydroxyapatite coating was lost during the processing phase; these areas were obvious and were not included in the analyses. The amount of HA coating was determined to average 57.95 ± 13.60% for specimens from patient 1, 52.24 ± 13.40% for specimens from patient 2, and 70.86 ± 9.15% for specimens from patient 3. The mean percentage of bone-HA coating contact for all specimens from the three patients was 48.31 ± 12.79%. The mean percentage of bone-cobalt alloy contact was 27.43 ± 11.77%. These regions showed contiguous

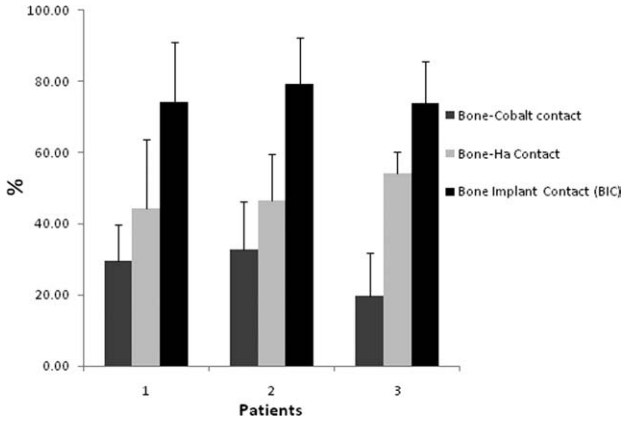

FIGURE 3. Histomorphometric results for all three patients. The percentage of bone in contact with HA coating was higher than the percentage of bone in contact with the CoCr implant where the coating was removed. All specimens from the three patients showed a BIC higher than 70%. Graph notation: "Patient 1" includes all specimens sectioned from patient 1; "Patient 2" includes all specimens sectioned from patient 2; and "Patient 3" includes all specimens sectioned from patient 3.

implant surface to bone without fibrous connective tissue within the limits of transmitted and reflected light optical microscopy. The average amount of total BIC for all specimens was 75.74 ± 13.74%. The results for specimens from each patient are shown in Figure 3.

Nanoindentation

The nanoindentation results for the specimens from each patient (mean and standard deviation) are shown in Table I. There was no data for elastic modulus and hardness at the bone-CoCr interface from specimens from patient 3; the limited absence of HA coating was difficult to resolve with the nanoindentation lens. Pooled data from all specimens are provided in Figure 4, which showed similar trends in modulus and hardness. The bone-HA coating indentations and the bone-CoCr indentations were not significantly different with respect to modulus ($p = 0.53$) and hardness ($p = 0.56$), and both averages were lower than for regions distant from the interface. The average elastic modulus of the bone at the HA-coating interfaces and at the bone-CoCr interfaces was 11.15 ± 3.25 GPa and 11.17 GPa ± 2.75, respectively. The average hardness of the bone at the HA-coating interfaces and at the bone-CoCr interfaces was 0.303 ± 0.105 GPa and 0.301 ± 0.087 GPa, respectively. The average modulus and hardness of bone distant to the implant interface was 16.59 ± 6.39 GPa and 0.411 ± 0.153 GPa, respectively. The differences in modulus comparing the area near (<200 μm) and distant (>1000 μm) were significant ($p = 0.04$), while the difference in the respective hardness values between these two regions was not ($p = 0.24$).

Backscattered electron imaging

BSE imaging along the implant interface showed qualitatively darker grey levels close to the CoCr implant interface [Fig. 5(A–C)] (which would correspond to lower relative density or degree of mineralization) as compared with regions distant from the interface, which appeared lighter (consistent with more mineralized bone). Several aligned osteons were observed [Figure 5 (A)] in regions adjacent to the interface. Bone adjacent to HA particulates appeared to be interstitial lamellar bone. Figure 5(C) shows a darker grey zone for bone adjacent to the HA coating and a variation in grey level in the areas between the two implant sections.

DISCUSSION

In this study, the implant-bone and coating-bone interfaces of relatively long-term functional hydroxyapatite-coated CoCr dental implants obtained post mortem were characterized. The primary intent of this study was to characterize the bone to implant interfaces. Any questions about clinical outcome aspects of these implants are referred to D.M. Martin. Implant-bone contact was established by histomorphometric analysis of the interfaces, while nanoindentation and backscattered electron imaging of bone near to and distant from the implant were utilized to study mechanical properties and provide qualitative assessment of bone mineralization, respectively. The results were consistent with the presence of relatively immature bone adjacent to the implants, which was less dense (lower mineralization) than the interstitial bone distant from the implant. These observations did not support our hypothesis that the bone located along the implant's HA interface would display mechanical properties comparable to bone distant from the implant. Instead, bone that was anatomically characteristic of remodeled bone which had occurred (probably several times) over a decade of *in vivo* function was observed. This finding suggests that bone immediately adjacent to these Custom Osseous Integrated Implants maintained structure and

TABLE I. Nanoindentation Modulus and Hardness Results for Each Patient

Patients	Modulus GPa < 200 μm Bone-HA Mean (SD)	Hardness MPa < 200 μm Bone-HA Mean (SD)	Modulus GPa < 200 μm Bone-CoCr Mean (SD)	Hardness MPa < 200 μm Bone-CoCr Mean (SD)	Modulus GPa > 1000 μm Distant Mean (SD)	Hardness MPa > 1000 μm Distant Mean (SD)
1	13.76 (4.90)	384 (172)	12.54 (5.06)	350 (173)	16.64 (5.61)	443 (209)
2	11.28 (4.89)	295 (151)	11.51 (4.77)	302 (172)	15.93 (5.16)	402 (183)
3	15.32 (5.61)	433 (249)	N/A	N/A	17.10 (4.97)	426 (233)
Pooled	13.07 (5.32)	359 (195)	11.90 (4.90)	321 (174)	16.41 (5.31)	422 (203)

"Patient 1" includes all specimens sectioned from patient 1; "Patient 2" includes all specimens sectioned from patient 2; and "Patient 3" includes all specimens sectioned from patient 3.

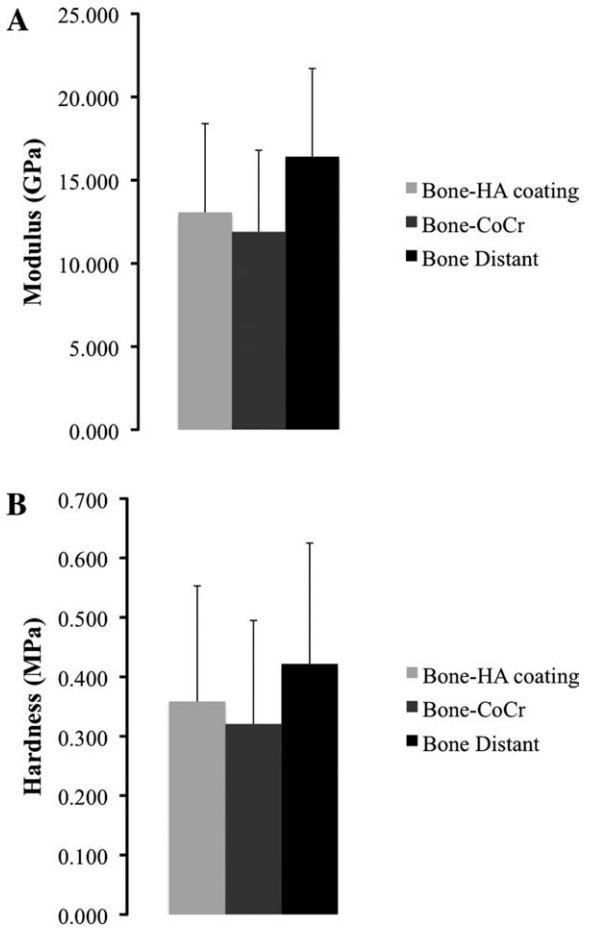

FIGURE 4. Nanoindentation results (pooled data). (A) Modulus (GPa) comparison for all specimens for the three patients. There was no significant difference between the modulus of the bone adjacent to the HA coating and the bone adjacent to the CoCr, but there was a significant difference when compared with modulus of bone distant (>1000 μm) to the implant interface. (B) Hardness (GPa) comparison for all three specimens showed the same trend as the modulus comparison but with no significant difference between values from bone near the interface (<200 μm) and bone distant (>1000 μm) from the interface.

biomechanical properties after about 11 years *in vivo*. The evolution of the bone interface properties over time remains to be determined.

To our knowledge, the present study is novel in its characterization of human bone-implant interfaces using the combination of nanoindentation, histomorphometry, and electron microscopy. These results are consistent with the aforementioned animal studies, in the detection of a significant difference ($p < 0.05$) in elastic modulus comparing bone "near" and distant" from implant interfaces.[1,24,26] The present results for nanoindentation hardness revealed a similar trend, with a lower average value near the interface, but this finding was not statistically significant. While

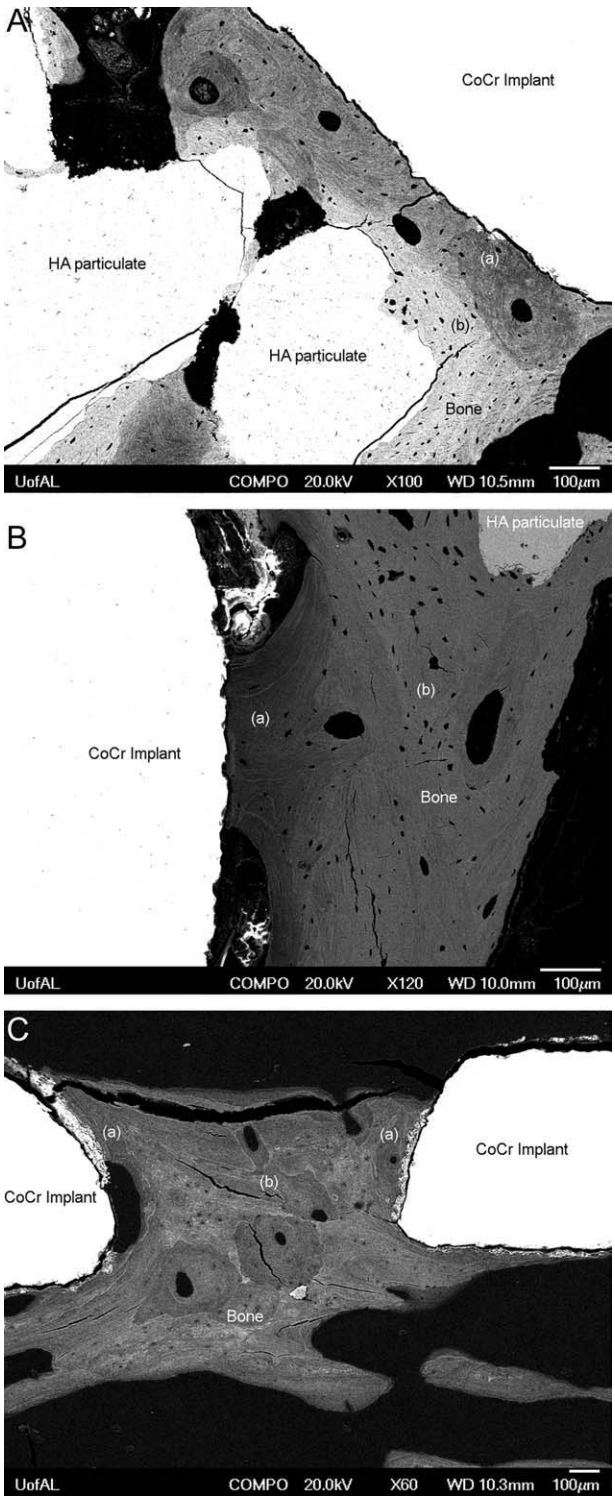

FIGURE 5. Backscattering electron imaging of the bone-implant interface. A: Image showing a darker grey level (lower mineral density) (a) in regions adjacent to the CoCr implant interface when compared to regions farther away from the interface (b). Also, it is noted that osteons are aligned in different orientations adjacent to the interface when compared to lamellar, interstitial bone seen in regions farther from the interface. B: Image showing another implant-interface area with a darker gray level in bone adjacent to the interface (a) when compared with bone farther from the interface (b). This region did not show aligned osteons in the interface, but the area shows a lighter gray level farther from interface (b). C: This bone-implant interface image of the bone area surrounding the HA coating showed a darker shade) (a) than areas of bone distant to the interface. There was variability in bone gray levels in the area between the two implants (b).

hardness and modulus have been shown to correlate in previous studies,[1,23] others have found that modulus better describes bone integration, because it determines stress and strain distribution around an implant that has been exposed to functional loading.[30,31]

The histomorphometric analyses showed that 52–70% of the implant surface was covered by HA coating after roughly 11 years *in vivo*. These percentages are higher than reported studies of different coatings at shorter *in vivo* periods.[13–16] The current data suggested that in regions where HA coating was no longer present, the coating was replaced by remodeled bone leading to direct contact along the CoCr surface of the implant. This result was different than previous studies which showed fibrous tissue adjacent to cobalt alloy surfaces for dental implants.[32–35] Additional studies will be needed to determine if any residues from the coating remained on the alloy. The average bone implant contact for all specimens averaged 75% integration and the bone surrounding the HA-coating and the CoCr demonstrated similar elastic modulus and hardness ($p > 0.05$). It appears, therefore, that the long-term implant status of integration was not affected by the HA-coating loss, consistent with studies done by others.[14,17,36,18,19]

The BSE images revealed substantial variability in bone grey levels (density) throughout the areas surrounding the implant and distant from the interface. There were images that clearly showed regions of darker grey near the interface [Fig. 5(A–C)]; however, other images showed variability in the degrees of grey level of bone between two implants and distant from the interface [e.g., Fig. 5(C)]. Bone grey levels (density) variation could be due to the heterogeneity of bone and the differences in mineralization, orientation, location, and specimen dimensions.

The present study provided novel data regarding bone properties surrounding HA-coated implants after about 11 years of function and new insight into the role of HA coatings on the nature of the bone-coating interface longer term. This study was limited in the use of specimens from only three donors, which were all women over 70 years of age. The observed differences in bone properties adjacent to the dental implants, therefore, may not be representative of the human population as a whole. The BSE images were not standardized using independent controls to correlate brightness and contrast throughout the specimens; therefore, the darker/lighter gray levels shown in the images could only be compared qualitatively within a sample, and were not used to numerically compare the bone densities between specimens. Further investigation using techniques such as electron dispersion x-ray spectroscopy may provide more quantitative evaluation of the bone structures analyzed in this study.

ACKNOWLEDGMENTS

Special thanks to Dr. Robin Foley from the Department of Materials Science and Engineering, Preston Beck from the Department of Prosthodontics from UAB, and Richard Martens and Johnny Goodwin from the Central Analytical Facility at the University of Alabama for their technical assistance. The donors and families of the patients are respectfully acknowledged.

REFERENCES

1. Chang MC, Ko CC, Liu CC, Douglas WH, DeLong R, Seong WJ, Hodges J, An KN. Elasticity of alveolar bone near dental implant-bone interfaces after one month's healing. J Biomech 2003;36: 1209–1214.
2. Sun L, Berndt CC, Gross KA, Kucuk A. Material fundamentals and clinical performance of plasma-sprayed hydroxyapatite coatings: A review. J Biomed Mater Res 2001;58:570–592.
3. Fujita H, Ido K, Matsuda Y, Iida H, Oka M, Kitamura Y, Nakamura T. Evaluation of bioactive bone cement in canine total hip arthroplasty. J Biomed Mater Res 2000;49:273–288.
4. Dickens SH, Kelly SR, Flaim GM, Giuseppetti AA. Dentin adhesion and microleakage of a resin-based calcium phosphate pulp capping and basing cement. Eur J Oral Sci 2004;112:452–457.
5. Walsh WR, Svehla MJ, Russell J, Saito M, Nakashima T, Gillies RM, Bruce W, Hori R. Cemented fixation with PMMA or Bis-GMA resin hydroxyapatite cement: Effect of implant surface roughness. Biomaterials 2004;25:4929–4934.
6. Kenny SM, Buggy M. Bone cements and fillers: A review. J Mater Sci Mater Med 2003;14:923–938.
7. Landor I, Vavrik P, Sosna A, Jahoda D, Hahn H, Daniel M. Hydroxyapatite porous coating and the osteointegration of the total hip replacement. Arch Orthop Trauma Surg 2007;127:81–89.
8. Cook SD, Thomas KA, Delton JE, Volkman TK, Whitecloud III TS, Kay JF. Hydroxylapatite coating of porous implants improves bone ingrowth and interface attachment strength. J Biomed Mater Res A 2004;26:989–1001.
9. Stephenson PK, Freeman MA, Revell PA, Germain J, Tuke M, Pirie CJ. The effect of hydroxyapatite coating on ingrowth of bone into cavities in an implant. J Arthroplasty 1991;6:51–58.
10. Cooley DR, Van Dellen AF, Burgess JO, Windeler AS. The advantages of coated titanium implants prepared by radiofrequency sputtering from hydroxyapatite. J Prosthet Dent 1992;67:93–100.
11. Rivero DP, Fox J, Skipor AK, Urban RM, Galante JO. Calcium phosphate-coated porous titanium implants for enhanced skeletal fixation. J Biomed Mater Res 1988;22:191–201.
12. Bloebaum RD, Merrell M, Gustke K, Simmons M. Retrieval analysis of a hydroxyapatite-coated hip prosthesis. Clin Orthop Relat Res 1991:97–102.
13. Tonino A, Oosterbos C, Rahmy A, Therin M, Doyle C. Hydroxyapatite-coated acetabular components. Histological and histomorphometric analysis of six cups retrieved at autopsy between three and seven years after successful implantation. J Bone Joint Surg Am A 2001;83:817–825.
14. Tonino AJ, van der Wal BC, Heyligers IC, Grimm B. Bone remodeling and hydroxyapatite resorption in coated primary hip prostheses. Clin Orthop Relat Res 2009;467:478–484.
15. MacDonald DE, Betts F, Doty SB, Boskey AL. A methodological study for the analysis of apatite-coated dental implants retrieved from humans. Ann Periodontol 2000;5:175–184.
16. Iezzi G, Degidi M, Scarano A, Petrone G, Piattelli A. Anorganic bone matrix retrieved 14 years after a sinus augmentation procedure: A histologic and histomorphometric evaluation. J Periodontol 2007;78:2057–2061.
17. Aebli N, Krebs J, Schwenke D, Stich H, Schawalder P, Theis JC. Degradation of hydroxyapatite coating on a well-functioning femoral component. J Bone Joint Surg Br 2003;85:499–503.
18. Overgaard S, Lind M, Josephsen K, Maunsbach AB, Bunger C, Soballe K. Resorption of hydroxyapatite and fluorapatite ceramic coatings on weight-bearing implants: a quantitative and morphological study in dogs. J Biomed Mater Res 1998;39:141–152.
19. Iezzi G, Orlandi S, Pecora G, Piattelli A. Histologic and histomorphometric evaluation of the bone response around a hydroxyapatite-coated implant retrieved after 15 years. Int J Periodontics Restorative Dent 2009;29:99–105.
20. Carlsson L, Regner L, Johansson C, Gottlander M, Herberts P. Bone response to hydroxyapatite-coated and commercially pure titanium implants in the human arthritic knee. J Orthop Res 1994; 12:274–285.

21. Rho JY, Tsui TY, Pharr GM. Elastic properties of human cortical and trabecular lamellar bone measured by nanoindentation. Biomaterials 1997;18:1325–1330.
22. Hoffler CE, Guo XE, Zysset PK, Goldstein SA. An application of nanoindentation technique to measure bone tissue Lamellae properties. J Biomech Eng 2005;127:1046–1053.
23. Zysset PK, Guo XE, Hoffler CE, Moore KE, Goldstein SA. Elastic modulus and hardness of cortical and trabecular bone lamellae measured by nanoindentation in the human femur. J Biomech 1999;32:1005–1012.
24. Huja SS, Katona TR, Moore BK, Roberts WE. Microhardness and anisotropy of the vital osseous interface and endosseous implant supporting bone. J Orthop Res 1998;16:54–60.
25. Oyen ML, Ko CC. Examination of local variations in viscous, elastic, and plastic indentation responses in healing bone. J Mater Sci Mater Med 2007;18:623–628.
26. Clark PA, Clark AM, Rodriguez A, Hussain MA, Mao JJ. Nanoscale characterization of bone-implant interface and biomechanical modulation of bone ingrowth. Mater Sci Eng C 2007;27:382–393.
27. Goldstein J, Newbury DE, Joy DC, Echlin P, Roming AD, Lyman CE, Fiori C, Lifshin E. Scanning Electron Microscopy and X-Ray Microanalysis. New York: Kluwer Academic/Penum Publishers; 2005.
28. Martin DM. Personal communication, 2008.
29. Oliver WC, Pharr GM. An improved technique for determining hardness and elastic modulus using load and displacement sensing indentation experiments. J Mater Res 1992;7:1564–1583.
30. Brunski JB. In vivo bone response to biomechanical loading at the bone/dental-implant interface. Adv Dent Res 1999;13: 99–119.
31. Turner CH, Forwood MR, Rho JY, Yoshikawa T. Mechanical loading thresholds for lamellar and woven bone formation. J Bone Miner Res 1994;9:87–97.
32. Linkow LI, Wagner JR, Chanavaz M. Tripodal mandibular subperiosteal implant: Basic sciences, operational procedures, and clinical data. J Oral Implantol 1998;24:16–36.
33. Moore DJ, Hansen PA. A descriptive 18-year retrospective review of subperiosteal implants for patients with severely atrophied edentulous mandibles. J Prosthet Dent 2004;92:145–150.
34. Minichetti JC. Analysis of HA-coated subperiosteal implants. J Oral Implantol 2003;29:111–116; discussion 117–119.
35. Amet EM. The mandibular subperiosteal implant denture: A prospective survival study. J Prosthet Dent 1996;75:347–348.
36. Bauer TW, Geesink RC, Zimmerman R, McMahon JT. Hydroxyapatite-coated femoral stems. Histological analysis of components retrieved at autopsy. J Bone Joint Surg Am 1991;73:1439–1452.